

Photonic Band Gap Micro-Cavities in Three-Dimension

Shawn-Yu Lin and J. G. Fleming

Sandia National Laboratories, P.O. Box 5800, Albuquerque, NM 87185

M.M. Sigalas, R. Biswas and K.M. Ho

Ames Labs, Department of Physics and Astronomy, Iowa State University, Ames, IA

50011

Abstract

Localization of light to less than a cubic wavelength, λ^3 , has important quantum consequences. The creation of single mode cavities and the modification of spontaneous emission are two important examples. A defect formed inside a three-dimensional (3D) photonic crystal provides an unique optical environment for light localization. Single mode defect cavities were built, for the first time, from an infrared 3D photonic crystal. A cavity state with modal volume of less than one λ^3 was observed.

Correspondence and requests for materials should be addressed to S.Y.L.
(e-mail:SLIN@sandia.gov)

DISCLAIMER

Portions of this document may be illegible in electronic image products. Images are produced from the best available original document.

A photonic crystal is the optical analogue of an electronic crystal [1-2]. It is an artificially engineered periodic structure with its dielectric constant spatially varied according to a certain crystal symmetry. Much like electrons in a crystal [3], photonic states inside a photonic crystal are classified into bands and gaps, frequency ranges over which photons are allowed or forbidden to propagate respectively. The bands and gaps provide a fundamentally new mechanism for localizing light to less than a cubic wavelength, λ^3 , which is not attainable using conventional optics [4-5].

A defect cavity may be used to trap light at a point within a three-dimensional (3D) photonic crystal. To create a point defect, dielectric function of a 3D crystal must be varied in a local region. Two general classes of defects may be made. One, the "vacancy defect", is created by removing a section of the dielectric material that comprises the 3D crystal. Another, the "interstitial defect", is formed by adding extra dielectric materials into the crystal. Within such a defect cavity, photonic defect state may appear in the otherwise forbidden photonic band gap regime, leading a strongly localized state [6]. The strength of photonic localization is determined by the size of the band gap, which acts as a highly reflecting mirror. To maximize the gap size, dielectric contrast (or equivalently refractive index) of the two materials that constitute the 3D structure and filling fraction of the higher dielectric material must be carefully chosen [7].

A layer-stacking design was used to construct the 3D photonic crystal. The design has been extensively studied theoretically and experimentally [7-10]. It consists of layers of one-dimensional rods with a stacking sequence that repeats itself every four layers. Within each layer the rods are parallel to each other and have a fixed pitch (d). The rod also has a fixed width (w) and height (h). The orientation of the rods on alternate layers is

rotated 90° between layers. Between every other layer, the rods are shifted relative to each other by an amount equal to half the pitch between the rods. For the special case of $4h/d=1.414$, the lattice can be derived from a faced-centered-cubic unit cell with a basis of two rods. The structure can also be derived by replacing the $\langle 110 \rangle$ chain of atoms in the diamond structure with the rods. For our 3D crystal, the maximum gap is achieved by having a index contrast of 3.6:1 and filling fraction of 28%. During the fabrication process, defect cavities can also be incorporated into a specific stacking layer. By varying the defect size, defect states may also be tuned across the band gap. In our case, vacancy defects are studied and their corresponding defect frequencies tuned by varying the length, L , of the removed section of the 1D rod.

To build the 3D crystal and defect cavities, a combination of advanced silicon processing techniques were used. In the first step of the process, a thin film of polysilicon is deposited, photopatterned and etched. The next step in the processing involves the use of chemical-mechanical-polishing (CMP) to planarize the patterned structure [10-11]. A layer of silicon dioxide (SiO_2) was deposited in between the lines of polysilicon. The wafers are then polished and planarized using CMP. The planarization step is critical since it prevents the topography generated in the first level from being replicated in the subsequent level. At this point the entire process is repeated to form a three layer structure. The fourth layer is a defect layer, where a series of vacancy defect is created having length $L=2, 15, \text{ and } 30 \mu\text{m}$. One top of the defect layer, three more layers were built to complete a seven layer 3D structure. After completion of the seventh layer, SiO_2 is removed by selective wet etching.

In Fig.1 (a), a cross section scanning electron microscopy (SEM) image of the defect

cavity is shown. The sample is cleaved right across the middle of the defect cavity for imaging purpose. The small missing section at the fourth layer is the defect cavity. A top view SEM image of the defect cavity at the fourth layer was shown in Fig.1(b). The defect is the small vacancy of length L along the 1D rod. The defect's geometric volume is given by $\Delta V = L \times 2d \times 3h$, where $L=2\mu\text{m}$, $d=4.3\mu\text{m}$ and $h=1.6\mu\text{m}$. Given the mid-gap wavelength of $\lambda \sim 11\mu\text{m}$, ΔV is as small as $\sim 0.06\lambda^3$. For cavities having $L=15$ and $30\mu\text{m}$, the corresponding ΔV is also compact: ~ 0.5 , and $1.0\lambda^3$ respectively. Additionally, defects are placed in an array fashion to maximize the transmission signal. Specifically, they are spaced by two rods along y -direction, a spacing distance of $3d=12.9\mu\text{m}$ (see Fig.1(b)), and separated by a distance Δx along x -direction.

To probe the localized states, both transmission and reflection measurements were carried out using a Fourier-transform infrared measurement system. Before measurement, the backside of the silicon substrate was polished to a smoothness of better than $0.2\mu\text{m}$ to avoid significant light scattering. To find the absolute transmittance (T), a transmission spectrum taken from a 3D crystal sample was normalized to that from a bare silicon wafer. To find the absolute reflectance (R), a reflection spectrum taken from the same 3D crystal is normalized to that of a silver mirror. Our reflectance set-up is capable of taking spectrum over an angular span of $\theta=15^\circ-70^\circ$ measured from the surface normal, i.e. $\langle 001 \rangle$ direction, and has an accuracy of $\pm 5\%$.

The absolute transmittance of light propagating through a 3D micro-cavity is shown in Fig. 2(a). The vacancy defect has a $L=2\mu\text{m}$, $\Delta x=10\mu\text{m}$, and $\Delta V \sim 0.06\lambda^3$. The infrared light is incident along the stacking direction, $\langle 001 \rangle$, of the 3D crystal and is un-polarized. The transmitted signal is collected by a photodetector with its receiving surface oriented along

$\langle 001 \rangle$ direction. A schematic drawing of the defect cavity (the dark square) and the transmission configuration is also shown in the inset. The transmittance shows a single transmission peak, centered at $\lambda_{\text{cavity}} = 12 \mu\text{m}$, indicating the existence of a cavity mode within the band gap. This transmitted signal originates from the resonant tunneling of electromagnetic waves through the single-mode cavity state. The peak transmission amplitude is $\sim 5\%$, or 13 dB, and full-width-half-maximum $0.8 \mu\text{m}$, or a cavity-Q of 15. The experimental data agrees with the result of a transfer matrix calculation [12-13] performed on a similar sample structure with $L = 2 \mu\text{m}$, $\Delta x = 12.9 \mu\text{m}$ [14]. In particular, it yields a $\lambda_{\text{cavity}} = 11.85 \mu\text{m}$ (indicated as an arrow), a slightly higher peak value of 8% and a cavity-Q of 20. The calculation also confirms that the defect cavity is a single mode resonant cavity.

The arrangement of defect cavities in an array fashion also allows us to probe wavefunction extent (localization length ε) of a defect state. When distance between adjacent defects is compatible to ε in the defect layer, near-by defects interact and defect modal frequency shifts. From the onset of this frequency shift, in-plane wavefunction extent may be estimated. This gives an experimental measure of the modal volume, ΔV_{mode} , associated with the defect cavity.

Transmittance spectra taken from defects arranged with defect spacing $\Delta x = 10, 15$ and $20 \mu\text{m}$ are shown in Fig.3. As expected, the defect frequency remains essentially the same for larger spacing samples, i.e. $\Delta x = 20$ and $15 \mu\text{m}$, and shifts to a longer wavelength of $\lambda = 12 \mu\text{m}$ for the $\Delta x = 10 \mu\text{m}$ sample. The shift to a longer wavelength is consistent with results of simulation, although it has a small uncertainty that comes from the uncertainty of the respective band edge positions, which is $\pm 0.05 \mu\text{m}$. Meanwhile, as Δx is reduced, defect density is increased and therefore the observed transmission amplitude is enhanced by about a factor of two. From the onset of the frequency shift, in-plane wavefunction extent of the defect cavity is estimated to be $\varepsilon_{//} \sim 10 \mu\text{m}$. The wavefunction extent along the stacking direction can also be obtained by performing transmittance measurement for samples with different number of layers [10]. By plotting transmittance as a function of

layer thickness, $\epsilon_z \sim 6\mu\text{m}$ is obtained [15]. From the known $\epsilon_{//}$ and ϵ_z , a cavity modal volume of $\sim 0.4 \lambda^3$ is deduced. This is, to the best of our knowledge, the smallest 3D defect cavity ever been made in the infrared wavelength.

Reflectance measurements are also carried out to study the optical properties of the defect. The spectrum was taken from the same sample at a slight tilt angle, $\theta=15^\circ$, and the measured data shown in Fig.2(b). The reflectance dip occurred at $\lambda_{\text{cavity}}=12\mu\text{m}$, which is consistent with the transmittance data. Unexpectedly, the amplitude of the observed dip is much more pronounced, $\sim 12\%$. It is about two times larger than the peak transmittance signal collected along $\langle 001 \rangle$. This observation suggests that some portion of the light may be scattered away from $\langle 001 \rangle$ and thus was not detected by the $\langle 001 \rangle$ oriented photodetector in the transmission configuration. The situation is quite different for a reflectance measurement since all resonant signals, scattered away or not, contribute to reflectance dip. A schematic for the scattering picture is shown in the inset of Fig.2(a). To confirm this hypothesis, a computer simulation that collect signals from all angles is carried out. The result shows that the integrated transmitted signal is indeed about two times larger than the $\langle 001 \rangle$ forward scattered one. It also indicates that surface scattering is not important and the source of scattering is the cavity itself. Such a scattering phenomenon is universal to both 2D and 3D photonic band gap micro-cavities [16].

To obtain a directional output for laser or light-emitting-diode applications, a special cavity design must be implemented to suppress the isotropic part of the scattering and thus enhance a more directional output coupling. One possible approach is to alter the detail of the modal wavefunction symmetry. This may be accomplished by either changing the geometrical shape of the cavity or through defect-to-defect interaction.

Reflectance measurements can also be used to verify the 3D nature of a defect cavity. If a cavity is truly three-dimensional, its modal frequency should be angular-independent. This is due to the fact that a 3D cavity mode is established by the coherent resonance of light, reflecting back from all facets of the cavity. A series of reflectance measurement was

carried out over an angle $\theta = 15^\circ - 70^\circ$ to investigate the angular dependence. Our results confirms that cavity frequency is angular independent for all angle tested and the defect cavity built from our 3D photonic crystal exhibits a 3D character.

Finally, a theoretical model calculation suggests that the excitation of the cavity mode is polarization dependent. The optical mode can only be excited by light polarized along the rod direction, i.e. the x-direction as indicated by the arrow in the inset of Fig.4. A schematic of the defect cavity is also shown in the inset. The defect cavity has a $L=30 \mu\text{m}$ and $\Delta x=50 \mu\text{m}$. The data taken with x-polarization, solid dots, shows a single transmission peak centered at $\lambda=11.3 \mu\text{m}$. The peak is well defined with its transmission amplitude of $\sim 7.5\%$, or 11dB attenuation, and full-width-half maximum $0.8 \mu\text{m}$, or a cavity-Q of 14. On the other hand, the data (open dots) taken with y-polarization shows no transmission peak in the gap regime, confirming the polarization-dependent of the cavity mode. The rejection ration, defined as the ratio of the transmittance between x- and y-polarization, is $\sim 10\text{dB}$. This value is limited by the polarization-independent evanescent leakage of light through the 7-layer structure which is about 1%. For a 10-layer defect cavity, rejection ratio is expected to be $\sim 20\text{dB}$. A vacancy defect can thus be used as a narrow band polarization selector.

In summary, single mode defect cavities were built, for the first time, from an infrared 3D photonic crystal. The defect state is polarization sensitive, shows a 3D character, and, most importantly, has an ultra-small modal volume of less than one λ^3 .

The authors gratefully acknowledge the expertise of the Sandia National Laboratories silicon processing team, especially P. Shea, A. Farino, D. Hetherington and B. Smith. The authors also thank Jim Bur and S.R. Kurtz for technical assistance. This work was supported by the United States Department of Energy under contract DE-AC04-94AL85000. Sandia is a multiprogram laboratory operated by Sandia Corporation, a Lockheed Martin

Company, for the United States Department of Energy.

References

1. See, for example, J.D. Joannopoulos, R.D. Meade and J.N. Winn, "Photonic Crystals", Princeton University Press, Princeton, New Jersey, 1995.
2. For the early theoretical investigation of three-dimensional photonic crystals, see: K.M. Leung and Y.F. Lu, *Phys. Rev. Lett.* 65, 2646-2649 (1990); Ho K.M., et al., *Phys. Rev. Lett.* 65, 3152-3155 (1990) and Z.Zhang & S. Satpathy, *Phys. Rev. Lett.* 65, 2650-2653 (1990).
3. See, for example, C. Kittel, "Introduction to Solid State Physics", Ch. 7, p.183-204, John Wiley & Sons, Inc., New York, N.Y., 1980.
4. E. Yablonovitch, *Phys. Rev. Lett.* 58, 2059 (1987).
5. S. John, *Phys. Rev. Lett.* 58, 2486 (1987).
6. E. Yablonovitch, et al., *Phys. Rev. Lett.* 67, 3380 (1991).
7. K.M. Ho et al., *Solid State Comm.* 89, 413-416 (1994).
8. S. Fan et al., *Appl. Phys. Lett.* 65, 1466-1468 (1994).
9. H. Sozuer & J. Dowling, vol. 41, 231-239 (1994).
10. S.Y. Lin, et al., *Nature*, Vol. 394, 251-253 (1998).
11. W.J. Patrick, W.L. Guthrie, C.L. Stanley and P.M. Schiabile, *J. Electrochem. Soc.* Vol. 138, 1778 (1991).
12. J.B. Pendry, *J. Modern Optics*, Vol. 41, p. 209 (1994).
13. E. Ozbay, et al., *Appl. Phys. Lett.* 64, 2059 (1994).
14. Our computer computation capability is limited to the case where Δx equals to integer number of the pitch a . In this case, $\Delta x=3a=12.9 \mu\text{m}$.
15. Here, ϵ_z is defined as the distance over which transmittance amplitude attenuated an amount of e^{-1} .
16. P. Vielleneuve, et al., *Phys. Rev. B* 54, 7837 (1996).

Figure Captions

Fig.1 A scanning electron microscopy (SEM) image of the defect cavity. (a) a cross section view of the vacancy defect with is at the fourth layer; (b) a top view of the defect cavity where $L=2\mu\text{m}$ and $a=4.3\mu\text{m}$.

Fig.2 (a) a transmittance spectrum of a 7-layer 3D micro-cavity taken with the infrared light propagating along the $\langle 001 \rangle$, or the z-direction, of the sample; the experimental configuration is shown in the inset. (b) a reflectance spectrum taken from the same sample at a slight tilt angle, $\theta=15^\circ$. The schematic drawing in the inset shows the scattering of light by the cavity.

Fig.3 Transmittance spectra taken from defects arranged with three different defect spacing $\Delta x=20, 15$ and $10\mu\text{m}$. The defect frequency remains essentially the same for both $\Delta x=20$ and $15\mu\text{m}$ and shifts significantly to a longer wavelength for $\Delta x = 10\mu\text{m}$.

Fig.4 The transmission spectra taken with x-polarization, shown as solid dots, and y-polarization, shown as open dots. The transmission peak is observed only for x-polarization, confirming the polarization dependence of a cavity mode.

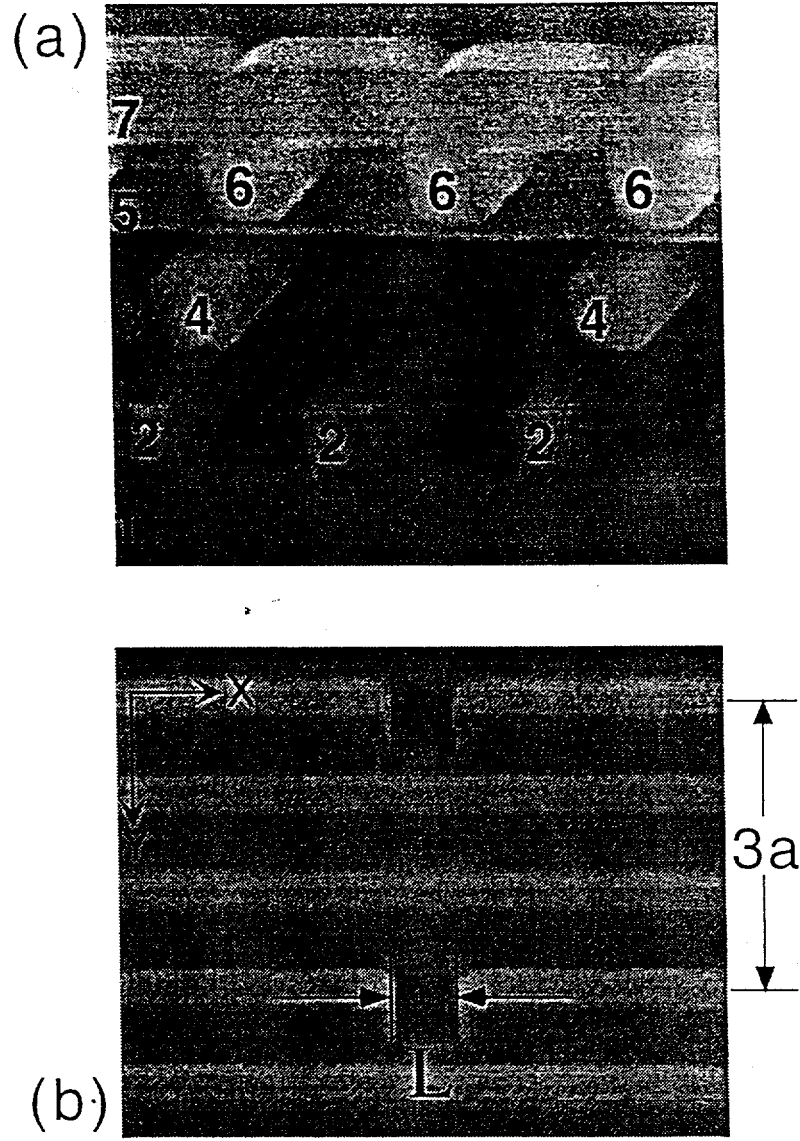


Fig.1

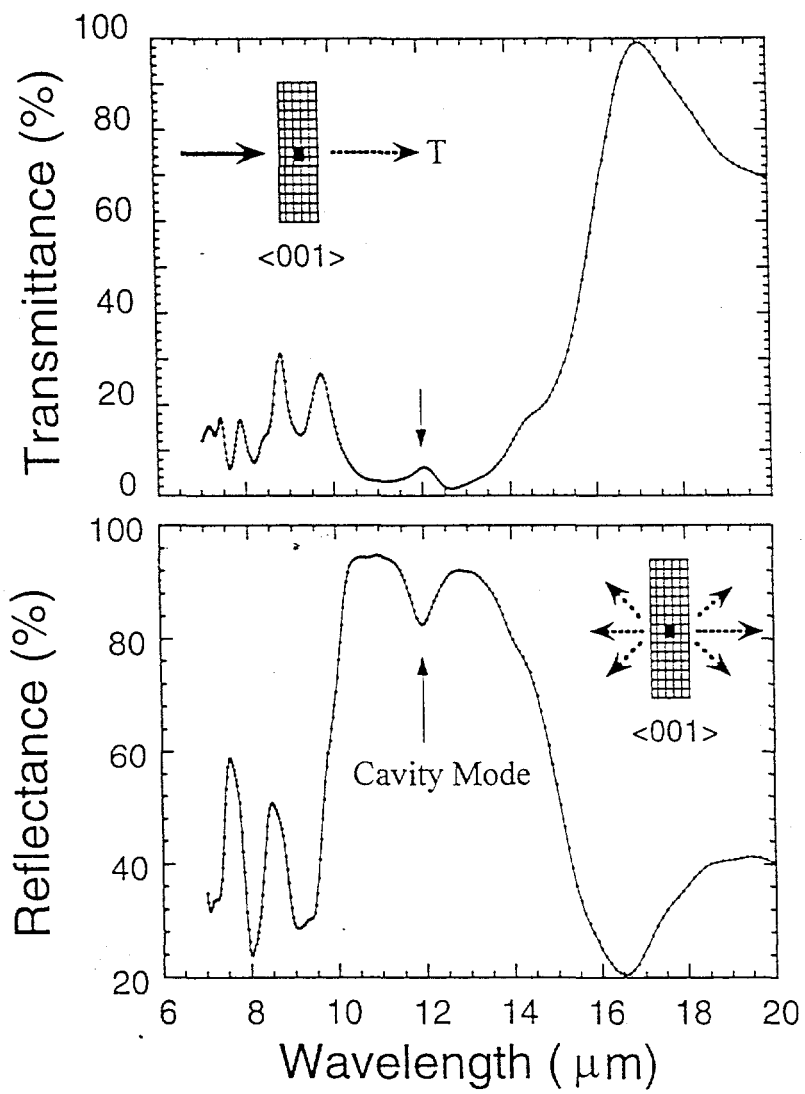


Fig.2

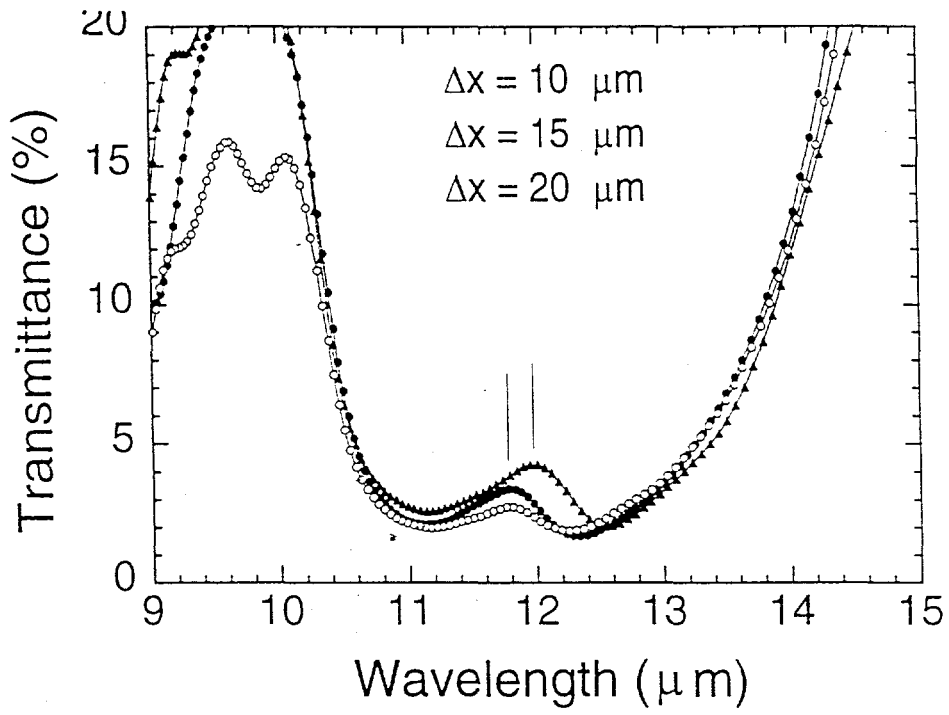


Fig.3

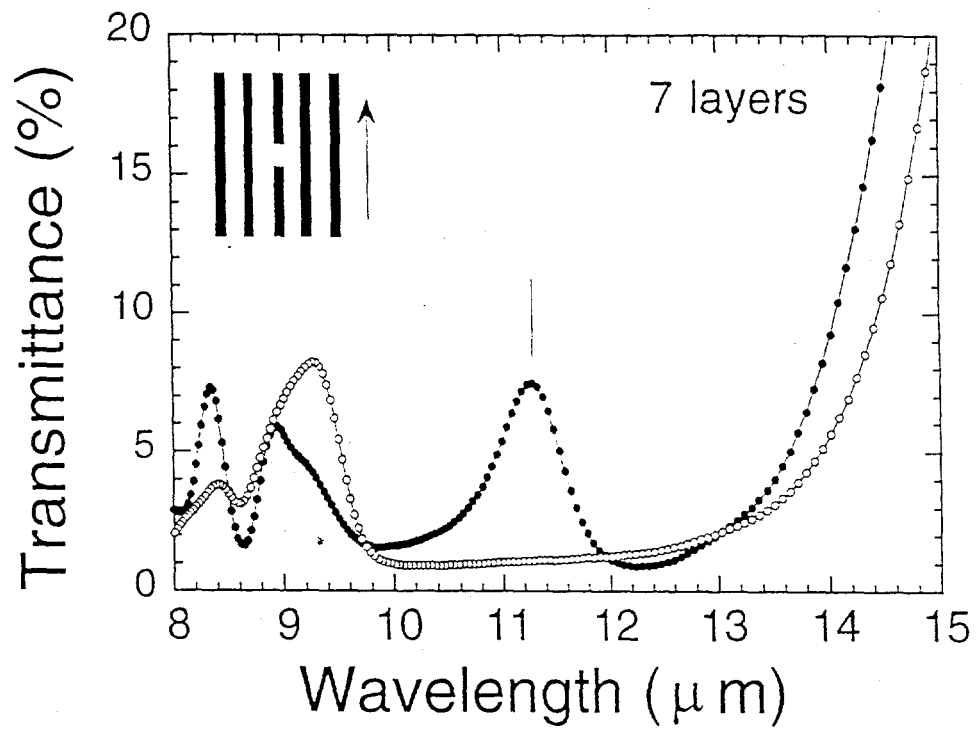


Fig.4